European Journal of Orthodontics 32 (2010) 242–247
doi:10.1093/ejo/cjp122
Advance Access Publication 18 December 2009

Accuracy of cephalometric landmarks on monitor-displayed radiographs with and without image emboss enhancement

Rosalia Maria Leonardi*, Daniela Giordano**, Francesco Maiorana*** and Mariagrazia Greco*
Departments of *Orthodontics **Computer Engineering and ***Informatics, University of Catania, Italy

SUMMARY The aim of this study was to evaluate the accuracy of some commonly used cephalometric landmarks of monitor-displayed images with and without image emboss enhancement. The following null hypothesis was tested: there is no improvement in landmark detection accuracy between monitor-displayed images, with and without image embossing enhancement.

Forty lateral cephalometric radiographs, taken from the data files of subjects were used in this study. A purpose-made software allowed recording of the cephalometric points and then, with the help of algorithms based on cellular neural networks, to transfer the previously processed radiographs into an embossed image. Five observers recorded 22 landmarks on the displayed images from the two image modalities, i.e. monitor-displayed radiograph (mode A) and monitor-displayed embossed radiograph (mode B). The positions of the landmarks were recorded and saved in the format of *x* and *y* co-ordinates and as Euclidean distance. The mean errors and standard deviation of landmarks location according to the two modalities were compared with the 'best estimate' for each landmark and the values were calculated for each of the 22 landmarks. One-way analysis of variance was then used to evaluate any statistically significant differences.

Euclidean distance mean errors were higher for the embossed images (except for Po) than for the unfiltered radiographs. These differences were all statistically significant ($P<0.05$) except for Or, Po, PM, Co, APOcc, and PPOcc. On the *x* and *y* co-ordinates, the accuracy of the cephalometric landmark detection improved on the embossed radiograph but only for a few points (Or on *x* axis and Po, PM, Co, and APOcc on *y* axis), as these were not statistically significant. The use of radiographic enhancement techniques, such as embossing, does not improve the level of accuracy for cephalometric points detection. Unless more precise algorithms are designed, this feature should not be used for clinical or research purposes.

Introduction

Image enhancements are a collection of processing techniques that seek to improve the visual appearance of digital images or transform the image into one more amenable to human and machine analysis. Enhancement techniques include: window and level selection, gamma correction, contrast manipulation, edge enhancement, subtraction, colourization, and embossing or three-dimensioanl (3D) reconstruction (Kogutt *et al.*, 1988; Crozier 1999; Menig 1999).

Embossing is the process of creating a 3D image starting from a two-dimensional (2D) image. Applying an embossing filter to an image often results in an image resembling paper or metal embossing of the original image, hence the name. The image obtained has sharpened edges and is graphically pleasing (Wiesemann *et al.*, 2006).

The use of enhancement techniques has proved to be beneficial in some radiographic applications (Jackson *et al.*, 1985; Kogutt *et al.*, 1988; Wiesemann *et al.*, 2006).

On this assumption, several software programs for cephalometric analyses have included sophisticated algorithms for image enhancement and facilitation of points for identification.

However, the use of enhancement algorithms for cephalometry has been questioned. In fact, even if they reduce random errors associated with landmark identification, the validity of the landmark may not be correct because of the introduction of systematic errors caused by the post-processing algorithms (Forsyth *et al.*, 1996; Menig, 1999).

Some of the drawbacks in these image enhancement techniques have been described, such as the enlarging tool (Jackson *et al.*, 1985; Kogutt *et al.*, 1988) and the edge enhancement technique (Forsyth *et al.*, 1996; Menig, 1999). However, little data are available on the clinical usefulness of digital cephalograms with emboss enhancement, even if it is perceived to improve clarity of cephalometric anatomical landmarks (Wiesemann *et al.*, 2006).

If enhancements are intended to reduce errors, increase accuracy, and simplify the process of extracting information, the enhanced images must provide perceptual information more suitable for locating landmarks than the original. Therefore, the aim of this study was to evaluate the accuracy of some commonly used cephalometric landmarks on monitor-displayed images with image emboss enhancement

and to compare findings with data obtained on the same monitor-displayed radiograph without any enhancement. The following null hypothesis was tested: there is no improvement in landmark detection accuracy between monitor-displayed images, with and without embossing.

Materials and methods

Forty lateral cephalometric radiographs, randomly selected from the data files of subjects attending the Department of Orthodontics, Catania University Hospital, were used in this study. The gender, type of occlusion, and skeletal pattern of the patients were not taken into consideration in the study design. The subjects were aged between 9 and 15 years of age (mean 13.9 years). Exclusion criteria were obvious malpositioning of the head in the cephalostat, unerupted or missing incisors and first molars, no unerupted or partially erupted teeth that would hinder landmark identification, patients with severe craniofacial deformities, and posterior teeth not in maximum intercuspation. Sample collection was approved by the University of Catania Research Ethics Committee and informed consent was obtained from each patient's parents before the study.

A power analysis suggested that a sample size of 40 radiographs was sufficient to evaluate significant differences in the accuracy of landmark detection with the two methods. In particular, the sample size ($N=40$) was chosen in such a way to obtain a power for the analysis of variance (ANOVA) test greater or equal to 0.8 for an estimated variance in landmark error equal to 0.1 mm and an effect size (difference between the mean with and without embossing) greater or equal to 0.065.

The cephalometric radiographs were scanned (Epson Expression 1680 Twain 2.10 Pro; Epson Italia S.p.A., Cinisello Balsamo, Italy) at a resolution of 300 dpi with 256 grey levels to transform the analogue image into a digital format using a scanner and stored in a PC (Intel Pentium IV, 3,2 GH with 2 GB RAM, 300 GB Hard Disk; ASUSTeK Computer Incorporated, Taipei, Taiwan) equipped with purpose-made software for cephalometric landmark recording. The software was designed and implemented in Borland C++ version 5.0 (Borland Software Corporation, Austin, Texas, USA) and allowed the recording of cephalometric points according to two modalities (mode A and mode B). Mode A consisted in landmarking the radiograph, which was shown on the screen without any kind of enhancement. In mode B, the software processed the same radiograph with algorithms based on cellular neural networks (CNNs; Giordano and Maiorana, 2007) and transformed it into an embossed image (Figure 1). The CNN is an unsupervised neural network that is computationally equivalent to a Turing machine and does not require training. By setting the values of two matrices, known as 'feedback' and 'control' templates, it is possible to implement any algorithm to manipulate the image (e.g. image filtering operations such as edge enhancement, embossing, morphological operations, etc.).

Prior to the study, the digitizer was checked for its accuracy according to a previous description (Macrì and Wenzel, 1993).

Twenty-two commonly used cephalometric landmarks were included in this analysis. Agreement between the five evaluators was reached on the definitions of landmarks before carrying out this study, and these written definitions for each landmark (Table 1) were given to evaluators. The observers were five orthodontists who were postgraduate trainers from the Orthodontic Department. The five observers recorded the 22 landmarks on the images displayed on the monitor from the two image modalities.

No more than 10 radiographs were traced in a single session to minimize errors due to examiner fatigue. Therefore, landmarking was carried out in eight sessions (40 images for mode A and 40 for mode B), with at least a 2 week interval between sessions. All recording sessions was performed in a dark room, the only available light being from the PC monitor. A 19 inch flat thin-film transistor screen (Samsung SyncMaster 913 V) set to an average resolution of 1280×1024 pixels, with bandwidths between 60 and 75 HZ, and a dot pitch of 0.294 mm, with standard setting: 80 per cent for contrast and 20 per cent for brightness. Landmark identification and recording directly on the monitor-displayed image was carried out with a mouse-controlled cursor. This cursor consisted of an arrow, and when a landmark was recorded, a red dot appeared on the screen over the selected pixel. The landmark position could be corrected until the operator was satisfied. Reference lines and perpendicular lines necessary to help identification appeared automatically on request. No time constraint was given to the users.

The positions of the landmarks were recorded and saved in the format of x and y co-ordinates with an origin fixed to one given pixel. For these monitor-displayed images, the construction of a x–y co-ordinate system was not necessary as the digital image consists of a pattern of rows and columns (the matrix) with an evenly spaced number of pixels in a known reference grid. The x and y co-ordinates were further analysed to evaluate the pattern of recording differences in the horizontal and vertical directions.

The mean x and y co-ordinate positions for each of 22 landmarks identified by the five observers, for the two modalities (mode A and mode B), were calculated and defined as the best estimate for that particular landmark in a given image. This best estimate was used to determine the inter-observer errors in both modalities, i.e. the digital image shown on the screen with and without image enhancement.

The mean distances in millimetres between the best estimate for each landmark and the mean of five locations identified by the five observers according to the two modalities were defined as inter-observer error. These were used as the variable determining accuracy for each landmark, with and without image enhancement.

a)

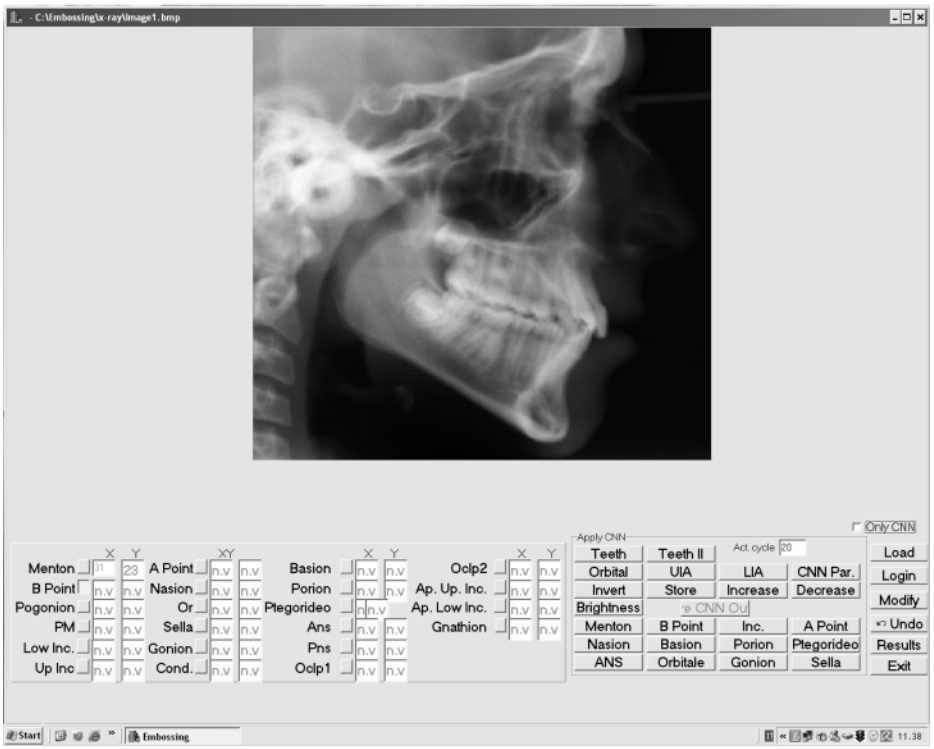

b)

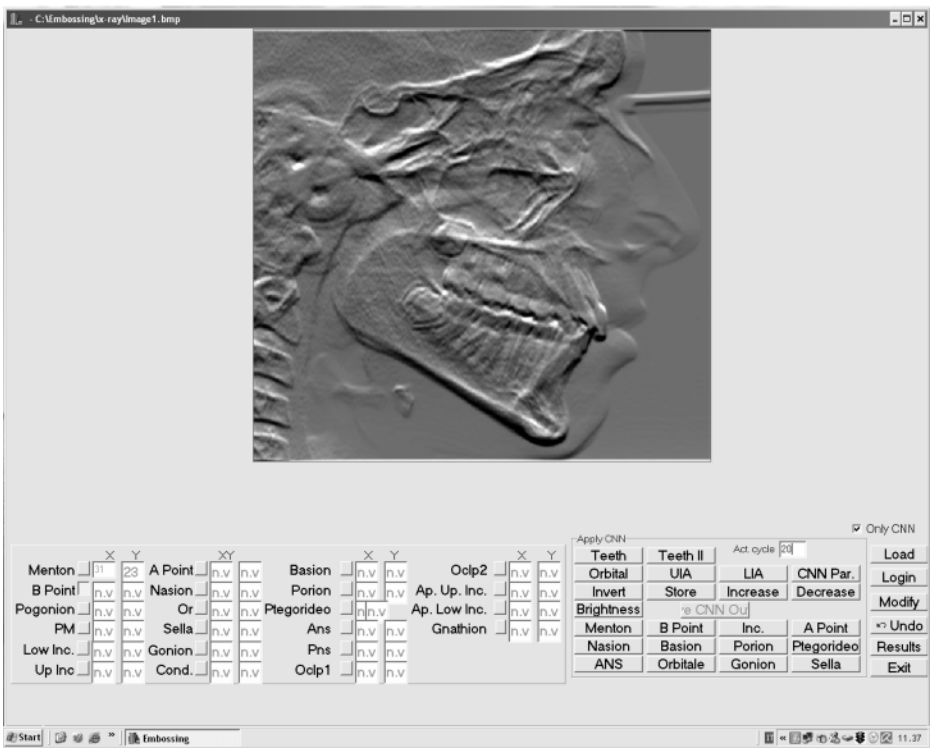

Figure 1 The interface of the landmarking tool: (a) an unfiltered and (b) an embossed radiograph.

Table 1 Definitions of landmarks.

Landmarks		
Name	Abbreviation	Definition
Nasion	Na	A point at the anterior limit of the nasofrontal suture.
Sella	S	Midpoint of the pituitary fossa as determined by inspection.
Orbitale	Or	A point located at the lowest point on the external border of the orbital cavity.
Porion	Po	A point located at the most superior point of the external auditory meatus.
Basion	Ba	The most inferior posterior point of the occipital bone at the anterior margin of the occipital foramen.
Pterygoid point	Pt	The intersection of the inferior border of the foramen rotundum with the posterior wall of the pterygomaxillary fissure.
Anterior nasal spine	ANS	Tip of anterior nasal spine.
Subspinale	A	The deepest point of the curve of the maxilla between ANS and the dental alveolus.
Posterior nasal spine	PNS	Tip of posterior nasal spine.
Supramentale	B	The deepest midline point on the mandible between infradentale and pogonion.
Protuberance menti or supra pogonion	PM	A point selected where the curvature of the anterior border of the symphysis changes from concave to convex.
Pogonion	Pg	Most anterior point on the midsagittal symphysis.
Gnathion	Gn	The most downward and forward point on the symphysis.
Menton	Me	The lowest point of the contour of the mandibular symphysis.
Gonion	Go	Intersection of the line connecting the most distal aspect of the condyle to the distal border of the ramus (ramus plane) and the line at the base of the mandible (mandibular plane).
Condylion	Co	The most postero-superior point on the outline of the mandibular condyle.
Upper incisor edge	UIE	Midpoint on the incisal edge of the most prominent upper central incisor.
Lower incisor edge	LIE	The incisal point of the most prominent mandibular incisor.
Upper incisor apex	UIA	The root apex of the most prominent upper incisor.
Lower incisor apex	LIA	The root apex of the most prominent lower incisor.
Anterior occlusal point	APOcc	The midpoint of the incisor overbite in occlusion.
Posterior occlusal point	PPOcc	The most distal point of the contact between the most posterior molar in occlusion.

Table 2 Mean error and standard deviation (SD), of the Euclidean distances (in millimetres), obtained from five observers' landmarking with (mode B) and without (mode A) enhancement from the 'best estimate' for each landmark.

Landmark	Mean error unfiltered image (A)	SD (A)	Mean error embossed image (B)	SD (B)	Difference (A − B)	*P*	One-way analysis of variance
Na	0.47	0.27	0.81	0.47	−0.34	0.00	*
S	0.33	0.15	0.46	0.21	−0.12	0.00	*
Or	1.52	0.86	1.57	0.86	−0.04	0.49	NS
Po	1.32	0.68	1.28	0.82	0.04	0.87	NS
Ba	0.91	0.48	1.21	0.62	−0.31	0.00	*
Pt	1.09	0.63	1.24	0.71	−0.16	0.05	*
ANS	0.55	0.31	0.68	0.35	−0.14	0.00	*
ANS	0.45	0.25	0.61	0.32	−0.17	0.00	*
PNS	0.72	0.45	1.17	0.63	−0.45	0.00	*
Ba	1.04	0.67	1.27	0.85	−0.24	0.00	*
PM	0.75	0.47	0.78	0.51	−0.03	0.63	NS
Po	0.51	0.31	0.63	0.35	−0.13	0.01	*
Gn	0.46	0.22	0.67	0.29	−0.21	0.00	*
Me	1.50	0.83	1.86	0.79	−0.36	0.00	*
Go	1.48	0.83	1.87	0.91	−0.39	0.00	*
Co	1.77	0.92	1.77	0.77	0.00	0.85	NS
UIE	0.24	0.12	0.71	0.42	−0.47	0.00	*
LIE	0.23	0.12	0.46	0.17	−0.23	0.00	*
UIA	0.94	0.49	1.08	0.58	−0.15	0.02	*
LIA	0.90	0.49	1.24	0.65	−0.34	0.00	*
APOcc	0.85	0.65	0.98	1.33	−0.13	0.57	NS
PPOcc	0.63	0.61	0.89	0.92	−0.25	0.15	NS

NS, not significant. *$P<0.05$.

Consequently, the accuracy of landmarks identification in each of the two modalities (monitor-displayed image with and without embossing) could be compared.

Statistical analysis

Mean errors and standard deviations of landmark location according to modes A and B were compared to the best

Table 3 Mean error and standard deviation (SD), on the *x* and *y* axes of the co-ordinate system (in millimetres), obtained from five observers' landmarking with (mode B) and without (mode A) enhancement from the 'best estimate' for each landmark.

Landmark	Mean error unfiltered image (A)	SD (A)	Mean error embossed image (B)	SD (B)	Difference (A − B)	*P*	One-way analysis of variance
NA X	0.23	0.18	0.34	0.24	−0.11	0.00	*
NA Y	0.40	0.30	0.74	0.55	−0.34	0.00	*
S X	0.17	0.11	0.30	0.22	−0.12	0.00	*
S Y	0.25	0.17	0.29	0.18	−0.04	0.02	*
Or X	1.43	0.90	1.33	0.95	0.10	0.34	NS
Or Y	0.41	0.30	0.70	0.42	−0.29	0.00	*
Po X	0.81	0.59	0.84	0.66	−0.04	0.95	NS
Po Y	1.01	0.63	0.97	0.75	0.05	0.87	NS
Ba X	0.46	0.32	0.88	0.66	−0.42	0.00	*
Ba Y	0.72	0.52	0.78	0.49	−0.06	0.15	NS
Pt X	0.39	0.31	0.42	0.31	−0.03	0.50	NS
Pt Y	0.94	0.69	1.12	0.75	−0.18	0.07	NS
ANS X	0.47	0.34	0.58	0.40	−0.12	0.00	*
ANS Y	0.22	0.15	0.26	0.17	−0.04	0.01	*
A X	0.20	0.14	0.29	0.19	−0.09	0.00	*
A Y	0.37	0.26	0.49	0.35	−0.12	0.00	*
PNS X	0.65	0.46	1.03	0.70	−0.39	0.00	*
PNS Y	0.20	0.14	0.51	0.32	−0.31	0.00	*
B X	0.20	0.15	0.23	0.17	−0.03	0.06	NS
B Y	1.08	0.73	1.29	0.90	−0.21	0.01	*
PM X	0.14	0.11	0.25	0.18	−0.11	0.00	*
PM Y	0.74	0.50	0.70	0.54	0.03	0.65	NS
Pg X	0.13	0.09	0.19	0.13	−0.05	0.00	*
Pg Y	0.48	0.34	0.57	0.38	−0.09	0.06	NS
Gn X	0.32	0.22	0.45	0.30	−0.13	0.00	*
Gn Y	0.27	0.20	0.40	0.30	−0.13	0.00	*
Me X	1.49	0.88	1.85	1.08	−0.36	0.00	*
Me Y	0.38	0.27	0.80	0.44	−0.42	0.00	*
Go X	0.81	0.56	0.89	0.57	−0.08	0.09	NS
Go Y	1.21	0.88	1.51	0.97	−0.30	0.00	*
Co X	0.96	0.61	0.99	0.63	−0.03	0.70	NS
Co Y	1.21	0.95	1.17	0.94	0.04	0.62	NS
UIE X	0.15	0.10	0.24	0.17	−0.09	0.00	*
UIE Y	0.16	0.13	0.63	0.45	−0.47	0.00	*
LIE X	0.13	0.09	0.23	0.17	−0.10	0.00	*
LIE Y	0.17	0.11	0.35	0.19	−0.18	0.00	*
UIA X	0.56	0.39	0.65	0.50	−0.09	0.09	NS
UIA Y	0.70	0.49	0.78	0.54	−0.08	0.15	NS
LIA X	0.61	0.45	0.91	0.64	−0.30	0.00	*
LIA Y	0.61	0.43	0.76	0.53	−0.15	0.01	*
APOcc X	0.43	0.54	0.56	0.97	−0.14	0.23	NS
APOcc Y	0.67	0.53	0.63	1.04	0.04	0.84	NS
PPOcc X	0.56	0.60	0.75	0.92	−0.19	0.29	NS
PPOcc Y	0.24	0.20	0.36	0.31	−0.12	0.04	*

NS, not significant. *$P<0.05$.

estimate for each landmark and values were calculated for each of the 22 landmarks, and differences were obtained. These were further analysed by ANOVA, to evaluate if they were statistically significant, in order to accept or reject the null hypothesis.

All statistical analyses were undertaken with the Statistical Package for Social Science (SPSS 16.0 release software Inc., Chicago, Illinois, USA).

Results

Table 2 reports, for each landmark, the Euclidean mean distance errors in millimetres and their standard deviations from the best estimate for each landmark, obtained for the five observers with and without image embossing. Table 3 shows the same data, but for each landmark co-ordinate (*x* and *y*).

The findings (Table 2) demonstrate that, in most instances, there were different mean distance errors between the embossed (mode B) and unfiltered (mode A) radiograph. The mean errors were higher for the embossed images (except for Po) than for the unfiltered radiograph. These differences were in most instances statistically significant ($P<0.05$).

The same pattern of errors was observed on the *x* and *y* co-ordinates, in fact accuracy on cephalometric landmark detection improved for the embossed radiograph only for a few points (Or on *x* axis and Po, PM, Co, and APOcc on *y*

axis) but these improvements were not statistically significant (Table 3). When comparing the mean distance errors between modes A and B, differences between the two methods were statistically significant ($P<0.05$) on the x co-ordinate for NA, S, Ba, ANS, A, PNS, PM, Pg, Gn, Me, UIE, LIE, and LIA and on the y co-ordinate for NA, S, Or, Po, ANS, A, PNS, B, Gn, Me, Go, UIE, LIE, LIA, and PPOcc.

Discussion

With the development of computer technology, it has become possible to 'capture' a radiographic image and to display this on a computer monitor as an array of small points (pixels), each with a particular shade of grey: the contrast and density of this image can be altered in the same way as a television picture. For example, it is possible to alter the radiograph image from negative to positive, manipulate contrast and brightness and alter the filter image. The perceived advantage of these techniques is that they can greatly facilitate landmark identification and therefore overall accuracy.

Some studies (Jäger *et al.*, 1989; Macrì and Wenzel, 1993; Wiesemann *et al.*, 2006) reported an improvement in image quality of digital cephalograms when using various digital enhancements and filtering techniques. However, this assumption is mostly based on observers' (raters') preferences of enhanced images over non-enhanced images and not if these enhancement affect the precision in landmark position identification.

Nevertheless, improved visual perception with manipulation of digital image does not necessarily mean an improved clinical performance. On this basis, the accuracy of landmark identification with and without the aid of emboss enhancement was evaluated in this study.

In most instances, embossing did not improve the accuracy of landmark detection both when considering Euclidean mean distance errors and errors from the x and y co-ordinate system. For several points, mean error differences were statistically significant. Higher mean errors from the 'best estimate' obtained for the embossed radiograph did not follow a specific pattern, as they were obtained both for points lying on edges and inside the skull. Therefore, it can be assumed that embossing filters introduce a random systematic error in the image (due, for example, to image distortion or edge erosion during processing), which negatively affects cephalometric point detection.

In the present study, several significant differences between the two image modalities, enhanced and non-enhanced images, were found. In all cases, an improvement of accuracy for emboss enhancement was observed. Thus, the null hypothesis is accepted.

Therefore, even though emboss enhancement is perceived to aid individual landmark clarity and also improve perception of overall image quality of cephalograms (Döler *et al.*, 1991; Wiesemann *et al.*, 2006), according to the findings of the present investigation, its use for clinical purposes cannot be recommended.

However, any enhancement techniques, as applied to cephalometry, have to be evaluated clinically.

Conclusions

The use of an embossing technique in cephalometry does not improve the level of accuracy of cephalometric point detection. Unless, more precise algorithms are designed, this feature should not be used for clinical and research purposes.

Address for correspondence

Dr Rosalia Leonardi
Department of Orthodontics
University of Catania
via S. Sofia n 78
Catania 95123
Italy
E-mail: rleonard@unict.it

References

Crozier S 1999 Is it time yet? Digital X-rays are here to stay, but how do you decide when to switch radiography systems? American Dental Association News, pp 28–32

Döler W, Steinhöfel N, Jäger A 1991 Digital image processing techniques for cephalometric analysis. Computers in Biology and Medicine 21: 23–33

Forsyth D B, Shaw W C, Richmond S, Roberts C T 1996 Digital imaging of cephalometric radiographs, Part 2: image quality. Angle Orthodontist 66: 43–50

Giordano D, Maiorana F 2007 A grid implementation of a cellular neural network simulator. 16th IEEE International Workshop on Enabling Technologies Infrastructure for Collaborative Enterprise (WETICE), Paris, France, pp. 217–222

Jackson P H, Dickson G C, Birnie D J 1985 Digital image processing of cephalometric radiographs: a preliminary report. British Journal of Orthodontics 12: 122–132

Jäger A, Döler W, Schormann T 1989 Digital image processing in cephalometric analysis. Schweizer Monatsschrift für Zahnmedizin 99: 19–23

Kogutt M S, Jones J P, Perkins D D 1988 Low-dose digital computed radiography in pediatric chest imaging. American Journal of Roentgenology 151: 775–779

Macrì V, Wenzel A 1993 Reliability of landmark recording on film and digital lateral cephalograms. European Journal of Orthodontics 15: 137–148

Menig J 1999 The DenOptix digital radiographic system. Journal of Clinical Orthodontics 33: 407–410

Wiesemann R B, Scheetz J P, Silveira A, Farman T T, Farman A G 2006 Cephalometric landmark clarity in photostimulable phosphor images using pseudo-colour and emboss enhancements. International Journal of Computer Assisted Radiology and Surgery 1: 105–112